Food Chemistry 315 (2020) 126270

Contents lists available at ScienceDirect

Food Chemistry

journal homepage: www.elsevier.com/locate/foodchem

Oxidative metabolism of typical phenolic compounds of Danshen by electrochemistry coupled to quadrupole time-of-flight tandem mass spectrometry

Juan Yang[a], Yan Chen[a], Xiao-Ting Zhen[a], Xin Dong[a], Li-Hong Ye[b,*], Hui Zheng[a,*], Jun Cao[a,*]

[a] College of Material Chemistry and Chemical Engineering, Hangzhou Normal University, Hangzhou 311121, China
[b] Department of Traditional Chinese Medicine, Hangzhou Red Cross Hospital, Hangzhou 310003, China

ARTICLE INFO

Keywords:
Danshen
Phenolic acids
Oxidative metabolism
Electrochemistry
Quadrupole time-of-flight tandem mass spectrometry

ABSTRACT

An electrochemistry coupled to online quadrupole time-of-flight tandem mass spectrometry (EC/Q-TOF/MS) was applied to investigate the oxidative transformation and metabolic pathway of five phenolic acids in Danshen sample. Simulation of the phase I oxidative metabolism was carried out in an electrochemical reactor equipped with a glassy carbon working electrode. The phase II reactivity of the generated oxidative products towards biomolecules (such as glutathione) was investigated by ways of covalent adduct formation experiments. The results obtained by EC/MS were compared with well-known in *vitro* studies by conducting rat liver microsome incubations. Structures of the electrochemically produced metabolites were identified by accurate mass measurement and previously results in *vivo* metabolites. It was indicated that the electrochemical oxidation was in good accordance with similar products found in *vivo* experiments. In conclusion, this work confirmed that EC/Q-TOF/MS was a promising analytical tool in the prediction of metabolic transformations of functional foods.

1. Introduction

Metabolic investigations are necessary for predicting and comprehending the metabolic stability of natural products in *vivo* and the possible interactions between the produced metabolites and the human body (Melles, Vielhaber, Baumann, Zazzeroni, & Karst, 2012). The most popular approaches of studying metabolism of natural products during experiments, include in *vitro* experiments using liver microsomes or perfused organs and in *vivo* experiments involving laboratory animal models (Brandon, Raap, Meijernan, Beijnen, & Schellens, 2003; Youdim & Saunders, 2010; Zhang, Luo, Ding, & Lu, 2012; Li et al., 2007). The metabolism processes are usually divided into two different phases. Phase I metabolism is mostly oxidation reactions, catalyzed in the liver by cytochrome P450 enzymes. The generated metabolite is not excreted directly by the kidneys or in the bile, or it can occur a Phase II reaction, in which nucleophiles, such as glutathione, are conjugated to the Phase I oxidation metabolites (Bussy, Chung-Davidson, Li, & Li, 2014; Iyer & Sinz, 1999; Li et al., 2007; Szultka-Mlynska & Buszewski, 2016). However, the use of animal models in *vivo* experiments involving scientific study and biological testing has caused concerns for the past many years among animal advocates (Arora et al., 2011). Due to time consuming, high cost, and multiple active compounds, there is great interest in developing rapid and simple metabolic simulation tools.

In the past several decades, the simulation of typical phase I oxidative metabolism using electrochemistry coupled with mass spectrometry (EC/MS) has achieved more attention (Getek, Korfmacher, McRae, & Hinson, 1989). The on-line EC/MS has been widely applied as a potential tool to deduce and predict redox reactions triggered with a single-electron oxidation mechanism, such as *N*-dealkylation, S- and P-oxidation, alcohol oxidation, aromatic hydroxylation and dehydrogenation (Jurva, Wikstrom, Weidolf, & Bruins, 2003; Jurva, Wikström, & Bruins, 2000). In biological systems, trapping agents like glutathione and proteins, are usually used to directly detect and identify highly electrophilic reactive metabolic intermediates (Mizutani, Yoshida, Murakami, Shirai, & Kawazoe, 2000; Melles, Vielhaber, Baumanna, Zazzeroni, & Karst, 2013). Lohmann et al. used EC/LC-MS to prepare reactive phase I oxidative metabolites of the drug, which further allowed to react with β-lactoglobulin A and human serum albumin (as a model protein) to form sufficient covalent adducts. (Lohmann, Hayen, & Karst, 2008). In comparison with chemical oxidation, EC/MS presented several advantages that there were nearly no need to remove reagents and oxidation products could be evaluated instantly after formation, so that short-living reactive oxidation products were detected before any reaction or rearrangement with other

* Corresponding authors.
E-mail addresses: yelihong81@163.com (L.-H. Ye), huizheng@hznu.edu.cn (H. Zheng), caoj@hznu.edu.cn (J. Cao).

https://doi.org/10.1016/j.foodchem.2020.126270
Received 17 October 2019; Received in revised form 16 January 2020; Accepted 19 January 2020
Available online 21 January 2020
0308-8146/

ingredient (Karady, Novák, Horna, Strnad, & Doležal, 2011). As far as we known, an attempt to use the technology to obtain information about potential oxidative transformation and metabolic pathway of natural products has rarely been reported so far.

Danshen (the root of *Salvia miltiorrhiza Bunge*), a well-known medicinal plant and functional food, has been widely used in the treatment of cardiovascular, cerebrovascular, liver and chronic renal failure diseases, especially angina pectoris, myocardial ischemia, coronary heart disease and stroke (Geng, Huang, Song, & Song, 2015; Sze, Yeung, Wong, & Lau, 2005; Sugiyama, Zhu, Takahara, Satoh, & Hashimoto, 2002). The main active compounds of Danshen were classified into two groups: hydrophilic phenolics and lipophilic diterpenoid quinines (Li, Song, Liu, Hu, & Wang, 2009). The former type was mainly constituted from the caffeic acid construction unit via various kinds of condensation reactions, including caffeic acid, danshensu, rosmarinic acid (RA), salvianolic acid C (Sal C), lithospermic acid (LA), salvianolic acid B (Sal B), etc (Jiang et al., 2005). In recent years, the hydrophilic compounds were considered as the phytochemical markers in the Chinese Pharmacopoeia 2015 due to various biological effects. The active water-soluble constituents of phenolic acids in Danshen are very complicated. Therefore, it is essential to illuminate the whole metabolic pathways of phenolic acids for a comprehensive understanding about the active constituents of Danshen. So far, most metabolic reports on phenolic acids have been carried out under different modes in *vivo*, including gut microflora, rat plasma, bile, urine, feces, WZS-pig urine (Bel-Rhlid et al., 2009; Nakazawa & Ohsawa, 1998; Jiang et al., 2012; Zhao et al., 2013; Yan, Lai, Li, & Chen, 2013; Wang et al., 2008; Miao et al., 2016). However, these investigations only focused on a single analyte or a few characteristic compounds of phenolic acids, which were insufficient to demonstrate the metabolic features of Danshen. In addition, the complex in *vivo* process after administration increased the difficulty in detection. Thus, a simple, fast and comprehensive EC/MS method is vital, which is proposed for a holistically metabolic study of multiple active constituents in Danshen.

In this work, electrochemistry coupled to online quadrupole time-of-flight mass spectrometry (EC/Q-TOF/MS) was presented as a simple, rapid method to investigate the oxidative transformation of characteristic phenolic acids (RA, protocatechuic aldehyde (PA), Sal C, LA, Sal B) in Danshen. Oxidation reactions were carried out in a three-electrode controlled-potential electrochemical reactor employing a glassy carbon electrode as the working electrode. High-resolution Q-TOF/MS was used to predict and elucidate the structure of intermediates and oxidation products. The generation and reactivity of metabolites and the possibility to simulate its biomolecule (glutathione) were also discussed. The obtained results were compared with a conventional in *vitro* microsomal approach with the use of rat liver microsomes (RLM), and in *vivo* assays, which indicated that it was a powerful tool in the investigation of the metabolic reactions of natural products.

2. Experimental

2.1. Chemicals

RA, PA, Sal C, LA, Sal B, were supplied by Shanghai Winherb Medical Technology Co., Ltd. (Shanghai, China). Chromatographic grade acetonitrile was obtained from Tedia Company Inc. (Fairfield, US). 20–22% ammonia was LC/MS grade supported by ANPEL Laboratory Technologies (Shanghai) Inc. (Shanghai, China). Glutathione (GSH) was obtained from Fluka (Buchs, Switzerland). Ammonium formate, sodium dihydrgen phosphate, disodium hydrogenorthophosphate and β-Nicotinamide adenine dinucleotide phosphate (β-NADPH) were all purchased from Sigma-Aldrich (Schnelldorf, Germany). Microsomes in *vitro* derived from male SD rat liver cells at the concentration of 10 mg/vial were obtained from Research Institute for Liver Diseases (Shanghai) Co. Ltd. (Shanghai, China). The microsomes were placed at −70 °C before experiments. Pure water was obtained by a Millipore Milli-Q purification system (Billerica, MA).

2.2. Instrumentation

The electrochemical oxidation of phenolic acids was performed in the ROXY™ system (Antec, Zoeterwoude, The Netherlands), which was committed to investigating the oxidative metabolism of drugs. EC was conducted in an electrochemical thin-layer cell (ReactorCell, Antec Leyden), which composed by a three-electrode arrangement, containing a glassy carbon working electrode, a Pd counter electrode and a HyREF (Pd/H_2) reference electrode. The glassy carbon electrode and the auxiliary electrode inlet module were separated by a 50 μm spacer, and the effective volume was 0.7 μL. The active surface area (wetted area) of the working electrode was approximately 14 mm^2, which was determined by the spacer. Potentials were ramped between 0 and 3000 mV using a dedicated ROXY potentiostat (Antec Leyden). Buffer solution was passed through the electrochemical cell by a syringe pump at a constant flow rate of 10 μL/min. The EC cell temperature was kept at 35 °C.

Mass analyses of the electrochemical products, were performed by a Q-TOF/MS from Agilent Technologies (Santa Clara, CA, USA) equipped with an Dual AJS electrospray ionization (ESI) source. Mass spectra were recorded in the negative ion mode under the following parameters: capillary voltage (V), 3500; drying gas temperature (°C), 350; nebulizer pressure (psig), 45; drying gas (N_2) flow rate (L/min), 12; fragmentor pressure (V), 175; OCT/RF (V), 750; skimmer voltage (V), 65. The mass-to-charge (m/z) ratio range was set from 100 to 1500. All the data were obtained and analyzed by Mass Hunter software (version B 08.00, Qualitative Analysis).

For all analyses of rat microsomal incubation, UHPLC/Q-TOF-MS separation was carried out on a ZORBAX SB C_{18} column (4.6 mm × 150 mm i.d., 5 μm, Agilent). During the separation process, the column constant temperature was kept at 35 °C and the flow rate of was set as 0.4 mL/min. The injection volume was 2 μL. The mobile phases were 0.1% formic acid in water and acetonitrile, and the corresponding gradient profile was shown below: 8%–20% B, 0–2 min; 20%–40% B, 2–4 min; 40%–80% B, 4–6 min; 80%–100% B, 7–8 min. The corresponding conditions for the Q-TOF/MS measurements were same as before.

2.3. Generation of metabolites by electrochemical oxidation.

20 mM ammonium formate buffer was prepared with water/acetonitrile (50/50, v/v) and used throughout the electrochemical experiments. For the electrochemical conversion, a 100 μM sample of target compound in a 20 mM buffer solution was used. The pH was adjusted to 7.4 with 20–22% ammonium hydroxide solution. A setup for on-line oxidation of metabolites by EC is shown in Fig. S1(a) (see Supplementary material). The samples were injected into the electrochemical flow-through cell at a constant flow rate of 10 μL/min with a syringe pump (1 mL glass syringe). The potentiostat was set to perform a potential scan from 0 to 3 V at a scan rate of 100 mV/s. Potential and time applied by the electrochemical cell are shown in Table S1. After electrochemical conversion of target analytes, the products were flowed to MS for real-time monitoring.

2.4. Adduct formation using GSH

For the investigation of target analyte trapping experiments with GSH, a slightly modification of EC/MS set-up was applied, as shown in Fig. S1(b). The electrochemical oxidation process was conducted under the same conditions mentioned above. After the electrochemical oxidation, 20 mM ammonium formate containing 300 μM GSH was added to the oxidized effluent of target analyte via a *T*-piece immediately. The GSH aqueous solution was constantly added at a flow rate of 10 μL/min via a syringe pump, resulting in the final flow of 20 μL/min to Q-TOF/

MS analysis.

2.5. Microsomal incubation

A mixture of RLM and target analytes was dissolved in 50 mM phosphate buffer solution at pH 7.4, and preincubated at 37 °C for 5 min in the constant total mixture volume of 500 μL. Whereafter, β-NADPH and magnesium chloride were added to the reaction mixture, which was then further placed in a warm water bath for 90 min at 37 °C. The final concentrations of incubation mixture were as follows: 1.3 mg/mL of RLM, 100 μM corresponding substrate (target analytes), 0.5 mM magnesium chloride and 1.2 mM NADPH. Subsequent to the incubation, microsomal proteins were precipitated by the addition of an equal volume (500 μL) of cold acetonitrile to the incubation mixture. After centrifugation at 13000 rpm for 5 min, the supernatant was analyzed by LC/Q-TOF/MS. To investigate the formation of covalent adducts between GSH and metabolites, additional incubation mixed solution with a concentration of 300 μM GSH wasprepared.

3. Results and discussion

3.1. Phase I oxidative metabolism simulation

3.1.1. Mass voltammograms of target analytes

Online EC/Q-TOF/MS has been applied to investigate the electrochemical oxidation products of target analytes, including RA, PA, Sal C, LA Sal B. A porous glassy carbon working electrode was used as electrochemical flow-through cell, whose high surface area was propitious to obtain a good conversion rate. In order to obtain a concise overview about oxidation behavior and the oxidation products of target analytes and to determine the optimal potential, a potential ramp from 0 to 3 V was applied to the electrochemical cell. The obtained three-dimensional plots were recorded by plotting continuously recording mass spectra vs. the applied potential. These allowed an identification of the generated potential oxidation products by increasing signal intensities of the corresponding *m/z* signals.

3.1.2. RA

In Fig. S2, a voltamperogram of RA obtained at different applied potentials is shown. In negative ion mode, oxidation of RA started at 0.4 V. Maximum yields for oxidation products were obtained at 0.7 V. The Mass spectrum obtained under optimized potentials is shown in Fig. S2, displaying an enlargement of the most interesting mass range between *m/z* 150 and 375. RA was determined as $[M-H]^-$ ion at *m/z* 359.08. With increasing potential, it was clear that the *m/z* ratios of RA was decreasing in intensity, stopping approximately at 0.7 V. By contrast, product signals with *m/z* 197.05 and 179.04 were increased, indicating generation of electrochemical oxidation products. Using a high-resolution Q/TOF-MS, the resulting molecular formulas were proposed based on their exact masses, which are depicted in Fig. 1. RA was oxidized to an electrochemical product at *m/z* 197.05 ($C_9H_{10}O_3$), which can be attributed to ester bond hydrolysis reaction. While the *m/z* ratio at 179.04 showed mass reduction by 18 Da, which was assigned to the loss of H_2O as a result of caffeic acid (intra molecular dehydration resulting in $C_9H_8O_4$).

3.1.3. PA

The 3D voltamperogram observed at glassy carbon working electrode potential swept from 0 to 1.2 V for PA as a target analyte is presented in Fig. S3. PA was easily characterized by the decreasing peak value at voltages higher than about 0.8 V. Simultaneously, its main proposed electrochemical products were generated, which presented increasing signal intensities at increasing voltages. Fig. S3 presents the mass spectra related to reactor cell with applied potentials of 0.6 V and 0.8 V. The mass spectrum for the mass-to-charge ratio (*m/z*) of PA as a target analyte (*m/z* 137.02) and its main oxidation products (*m/z* 151.00 and 245.05), created at different levels of voltage (0.6 V and 0.8 V). An overview of electrochemical oxidation products is described in Fig. 2. Products formed by proposed electrochemical oxidation of PA was divided into different groups, including methylation (*m/z* 151.00), dimethylation and sulfation (*m/z* 245.05).

3.1.4. Sal C

The mass spectrum for the *m/z* of Sal C as a target analyte and its main proposed electrochemical products, created at different values of potential ranged from 0 to 3 V, are shown in Fig. S4 as a 3D MS voltammogram. The obtained mass spectra revealed multiple signals of varying intensity coming from stable and unstable Sal C derivatives. The molecular ion of Sal C had a *m/z* of 491.10 and its intensity, as illustrated in Fig. S4, decreased when the oxidation potential surpassed 0.5 V, which indicated the oxidation. The highest signal intensity was observed for the oxidation product at 2.5 V. According to the mass gain of 13 and 45 from the parent substance Sal C (*m/z* 491.10), the product *m/z* 504.09 and 536.08 were attributed to a formal addition. Details for the oxidation process of Sal C are discussed in detail in Fig. 3. The *m/z* ratios 504.09 and 536.08 presumably derived from the addition of methylation and carboxylation to Sal C.

3.1.5. LA

In order to obtain first insight into the phase I electrochemical oxidation behavior of LA and to detect the optimal voltage for further EC/MS studies, mass voltammogram of LA was generated (presented in Fig. S5) using glassy carbon as working electrode. LA itself was detected at *m/z* 493.12 as $[M-HCOOH]^-$. Products of LA formed by electrochemical oxidation were easily identified by the increasing peak intensity at voltages higher than approximately 1.2 V. As shown in Fig. S5, the $[M-H]^-$ ion of LA oxidation product with *m/z* 550.10 was observed with small signal, beginning at approximately 1.2 V. The oxidation reactions occurring in the electrochemical reactor are depicted in Fig. 4. A decarboxylation of *m/z* 537.07 led to a product at *m/z* 493.12. Besides, a further oxidation to a methylation product was observed at *m/z* 550.10.

3.1.6. Sal B

As shown in 3D plot ramped from 0 to 1.3 V for Sal B (Fig. S6), the conversion of Sal B into phase I electrochemical oxidation products was successfully obtained. The Sal B molecule could easily be deprotonated and detected with high signal as $[M-H]^-$ ion (*m/z* 717.14) in the negative ionization mode of the Q-TOF/MS. The graph (Fig. S6) presents that for the voltage values 0.6 and 1.2 V, the value of the signal at *m/z* 717.14, which is originating from the unchanged target analyte structure, is still very high compared with the value of other signals (*m/z* 731.13, 745.11) belonging to Sal B oxidation products. Based on the EC/MS experiments and information available in the previous reports, the corresponding oxidation product structures are deduced in Fig. 5, which are discussed further. Presumably *m/z* 731.13 has been formed from Sal B via a methylation reaction, exhibiting ions with an *m/z* increased by 14 Da. As this *m/z* ratio was 28 Da higher than 717.14, it could be assumed that it came from a dimethylation of Sal B, the corresponding of *m/z* 745.11.

3.2. Phase II oxidative metabolism simulation

3.2.1. RA

GSH was a momentous trapping agent for reactive products generated in *vivo* during the phase II metabolism. The electrochemical behavior of RA in the presence of GSH at applied voltages of 0 and 0.7 V was studied, as shown in Fig. S2. When RA was oxidized electrochemically at 0.7 V and the effluent of the electrochemical cell was mixed online with GSH via a *T*-piece, three different adducts with GSH were observed by accurate mass data. The signal intensities of RA and GSH presented decreasing whereas increasing intensities for the found

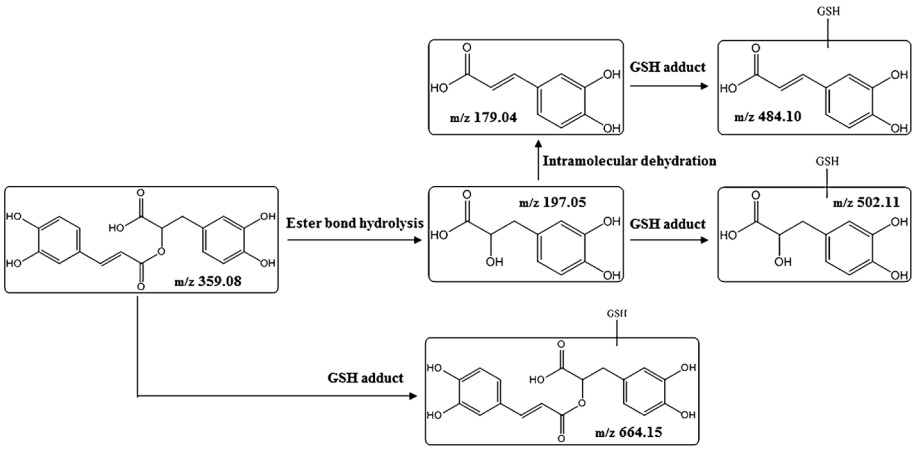

Fig. 1. Metabolism pathway for the electrochemical oxidation of RA.

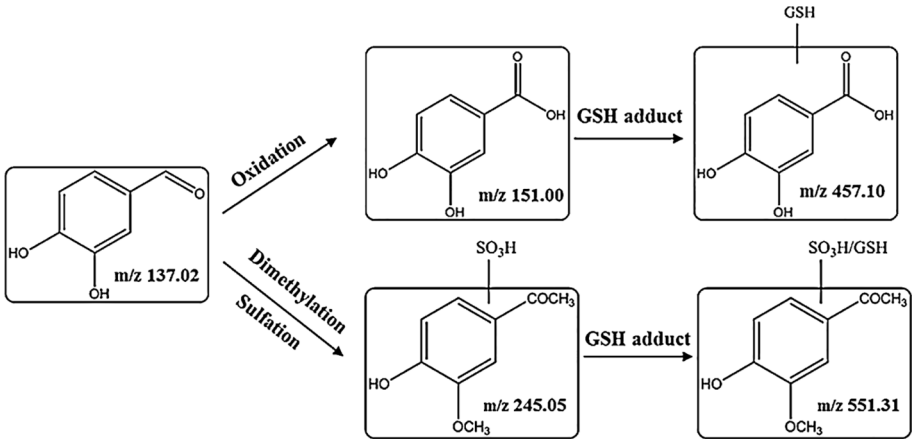

Fig. 2. Suggested structures and reactions for PA and its oxidation products.

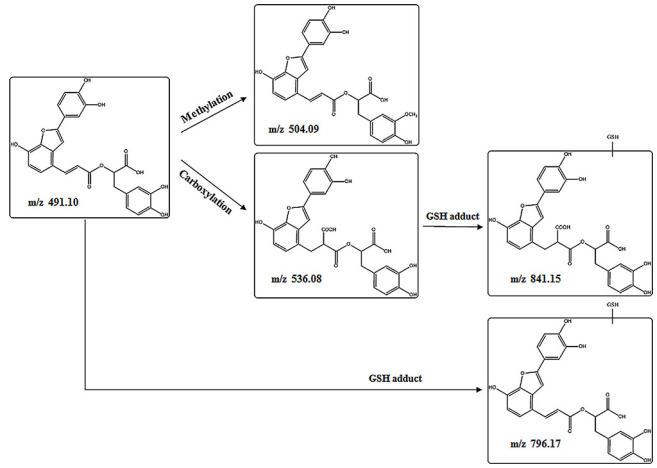

Fig. 3. Proposed transformation pathway of Sal C with the most abundant electrochemical products and GSH adducts.

electrochemical oxidation adducts were obtained. Adduct formation of reactive intermediates related to a Michael-type addition of GSH, e.g., RA (*m/z* 359.08) and its electrochemical oxidation products, 3,4-Dihydroxyphenyllactic acid (*m/z* 197.05) and caffeic acid (*m/z* 179.04). It was possible to obtain stable electrochemical oxidation adducts with *m/z* 484.10 (affeic acid + GSH) *m/z* 502.11 (3,4-Dihydroxyphenyllactic acid + GSH) and *m/z* 664.15 (RA + GSH) for phase II of metabolic transformation (Fig. 1).

3.2.2. PA

To clarify the reactivity of the electrochemically produced oxidation products towards GSH, PA was oxidized and the related products were allowed to react with GSH. Fig. S3 shows the mass spectrum of these adducts formed at high voltages (0.6 V and 0.8 V) at the surface of glassy carbon electrode. GSH was reactive towards PA oxidation products, and two covalent GSH adducts were generated as could be theoretically expected. Minor signals at *m/z* 457.10 and 551.31 corresponded to adducts with GSH. GSH adducts with a *m/z* ratio of 457.10, relating to the reaction of the above mentioned methylated PA (*m/z* 151.00) with GSH. The signal at *m/z* 551.31 can be ascribed to the reaction of dimethylation and sulfation oxidation product of PA (*m/z* 245.05) with GSH, as was described before (Fig. 2). The results of the electrochemical oxidation adducts of PA were in good agreement with the assumption of Michael-type addition.

3.2.3. Sal C

From the systematic observation of GSH adducts, electrochemistry can be used for the simulation of Sal C oxidation products formation and its binding to biomolecules (e.g., GSH), and both of which can be observed by accurate mass spectrometry (Fig. S4). It was indicated that Sal C and oxidation products were completely trapped by GSH, and two GSH adducts with *m/z* 796.17, 841.15 were generated. The mass spectrum was obtained when the electrochemical cell switched off (0 V), which made it possible to initiate a reaction that resulted in creating a signal coming from a GSH adduct at *m/z* 796.17. The GSH conjugate with *m/z* 796.17, can likely be attributed to reaction of Sal C with GSH. The signal at *m/z* 841.15 can be assigned to a GSH adduct of the Sal C carboxylation product mentioned above (*m/z* 536.08, Fig. 3).

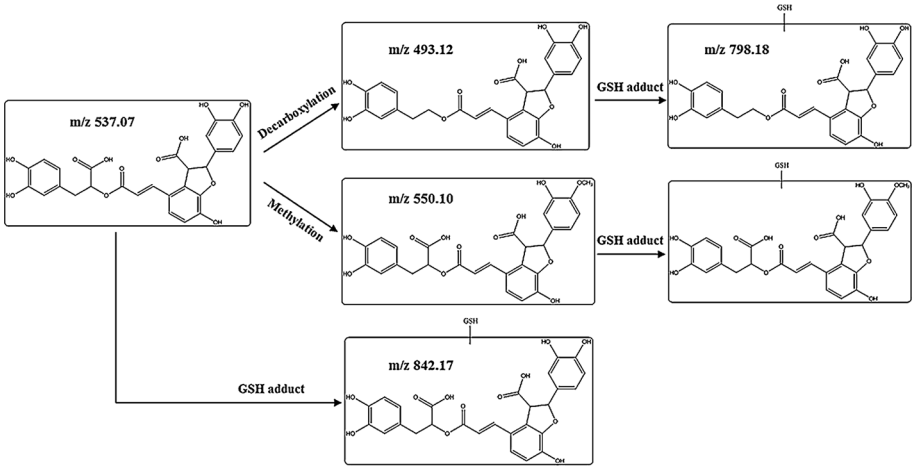

Fig. 4. EC/MS-based prediction of the oxidative metabolites and GSH adducts of LA.

3.2.4. LA

For assessing the reactivity of the electrochemically produced oxidation products of LA towards GSH, the reaction of those reactants was started via a *T*-piece. The starting potential of electrochemical conjugation of LA (as a model compound) in the EC cell was 0 V. The mass spectrum of the target analytes at constant potentials of 0.7 and 1.7 V was then described to observe the additional peaks of the electrochemical adducts. When on-line EC/MS was run with the electrochemical reactor switched off, only the peak at *m/z* 493.12 (deprotonated LA) was observed (as shown in Fig. S5). At 0.7 V and 1.7 V, two possible peaks were generated, including those of the adducts at *m/z* 798.18 and 842.17. The peak at *m/z* 798.18 indicated the adduct of decarboxylation LA and GSH, while *m/z* 842.17 could be attributed to the GSH adduct of deprotonated LA (see Fig. 4).

3.2.5. Sal B

Further experiments were carried out under the same experimental conditions except in the presence of GSH. The electrochemical oxidation products of Sal B conjugate with GSH, creating phase II derivatives. Potential adducts between the electrochemical oxidation products of Sal B and GSH were identified by emerging *m/z* signals from mass spectrum. As demonstrated by the observation of Fig. S6, it was possible to reveal potential conjugation reactions, including *m/z* 1022.21 was generated with high signal intensities, and the adduct *m/z* 1036.19 was observed with a relatively low intensity. The GSH conjugate with *m/z* 1022.21, resulted from adduct of the GSH and Sal B. The signals with *m/z* 1036.19 was likely be explained as the adduct of methylated Sal B and GSH. The expected mechanism related to a Michael addition, which led to the structures shown in Fig. 5.

3.3. In vitro investigations with RLM

With the purpose of a comparison of the electrochemical oxidation results with conventional methods for metabolism simulation, the proposed metabolic pathways through the incubation with RLM, was carried out. Based on EC/MS oxidation results, RLM incubations of RA, PA, Sal C, LA, Sal B and their GSH conjugations were applied and analyzed by means of LC/MS. The corresponding extracted ion chromatograms of the metabolites detected in the RLM incubation mixtures, obtained after LC/MS analysis, are shown in Fig. S7. It should be noted that the *vitro* studies with RLM showed strong similarities with the purely electrochemical instrumental method since it was possible to form major metabolites in the EC reactor, including several electrochemical oxidation adducts. As predicted by EC/MS, 3,4-Dihydroxyphenyllactic acid (*m/z* 197) and caffeic acid (*m/z* 179) were predominantly generated by the liver microsomes of rats. After a 90 min incubation of RA with GSH, the GSH adduct with *m/z* 484 and 502 were also appeared in the chromatogram. Compared to EC/MS, four metabolites, methylated PA (*m/z* 151), dimethylation and sulfation oxidation product of PA (*m/z* 245) and their GSH adducts (*m/z* 457 and 551), were found after the RLM microsomal incubation. For *m/z* 491 and 503, detected in the LC/MS analysis of Sal C microsomal approach, it was suggested that it was prototype and methylation product of Sal C. Since GSH was added to the incubation mixture, additional extracted ion

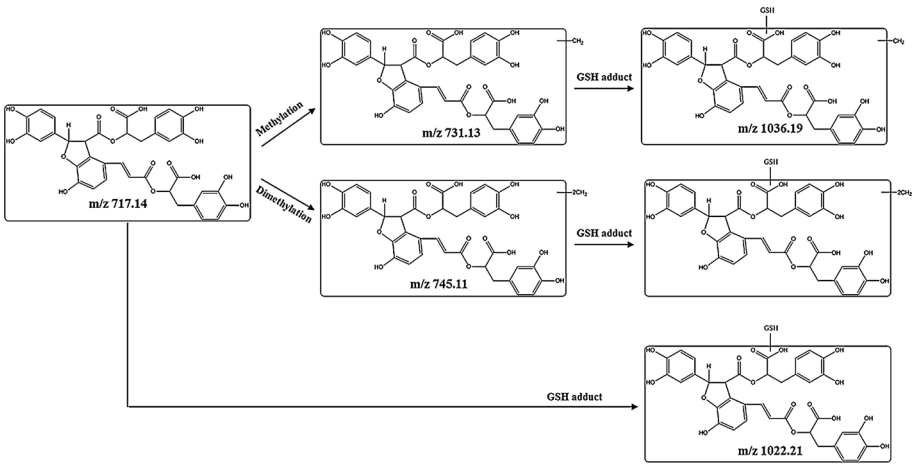

Fig. 5. Proposed oxidation products and GSH adducts of Sal B in the EC Cell determined by the Q-TOF/MS.

Table 1
Compounds identified from different metabolic modes of phenolic acids for Danshen.

Analytes	Metabolic mode	Metabolites *m/z*	Identification	References
RA				
1	Gut microflora	*m/z* 179	Caffeic acid	Bel-Rhlid et al. (2009)
		m/z 197	3,4-Dihydroxyphenyllactic acid	
2	Rat urine	*m/z* 259	Trans-caffeic acid 4-O-sulfate	Nakazawa and Ohsawa (1998)
		m/z 243	Trans-m-coumaric acid 3-O-sulfate	
		m/z 273	Trans-ferulic acid 4-O-sulfate	
		m/z 179	Trans-caffeic acid	
		m/z 165	m-hydroxyphenylpropionic acid	
		m/z 163	Trans-m-coumaric acid	
		m/z 359	unchanged RA	
3	EC/MS	*m/z* 179	Caffeic acid	This method
		m/z 197	3,4-Dihydroxyphenyllactic acid	
		m/z 359	unchanged RA	
PA				
1	Rat urine	*m/z* 217	PA sulfate	Jiang et al. (2012)
		m/z 231	PA methylated sulfate	
2	WZS-miniature pig urine	*m/z* 329	Protocatechuic acid glucuronide	Zhao et al. (2013)
		m/z 313	PA glucuronide	
		m/z 218	4-Hydroxymethyl-1,2-benzenediol sulfate	
		m/z 245	apocynin sulfate	
3	EC/MS	*m/z* 151	Methylated PA	This method
		m/z 245	PA dimethylated sulfate	
Sal C				
1	Rat plasma and urine	*m/z* 179	Caffeic acid	Yan et al. (2013)
		m/z 681	Methylated Sal C glucuronide	
		m/z 695	Dimethylated Sal C glucuronide	
		m/z 519	Dimethylated Sal C	
2	EC/MS	*m/z* 504	Methylated Sal C	This method
		m/z 536	Carboxylated Sal C	
LA				
1	Rat serum and bile	*m/z* 551	3′-monomethyl-LA	Wang et al. (2008)
		m/z 565	3′,3″-dimethyl-LA	
2	Rat plasma, bile, urine and feces	*m/z* 551	Methyl LA	Miao et al. (2016)
		m/z 565	Dimethyl LA	
3	EC/MS	*m/z* 493	Decarboxylated LA	This method
		m/z 551	Methyl LA	
Sal B				
1	Rat plasma, bile, urine and feces	*m/z* 731	Methyl Sal B	Miao et al. (2016)
		m/z 745	Dimethyl Sal B	
		m/z 759	Trimethyl Sal B	
		m/z 797	Sal B sulfate isomer	
		m/z 811	Methyl Sal B sulfate	
		m/z 825	Dimethyl Sal B sulfate	
		m/z 839	Trimethyl Sal B sulfate	
2	Rat biliary	*m/z* 759	3,3″,3‴-O-tri-methyl-Sal B	Xu et al. (2007)
		m/z 731	3-O-monomethyl-Sal B	
		m/z 745	3,3″-O-dimethyl-Sal B or 3,3‴-O-dimethyl-Sal B	
	Rat fecal	*m/z* 197	(s)-3-(3,4-dihydroxyphenyl) lactic acid or Danshensu	
		m/z 361	Salvianolic acid R (Named by the author)	
		m/z 539	Salvianolic acid S (Named by the author)	
		m/z 539	Salvianolic acid T (Named by the author)	
3	EC/MS	*m/z* 731	Methyl Sal B	This method
		m/z 745	Dimethyl Sal B	

chromatograms (*m/z* 796 and 841) were formed in expectations. The metabolic pathway of LA by microsomal incubation included the formation of decarboxylation and methtylation products of LA (*m/z* 493, 551), followed by a conjugation reaction of LA with GSH (*m/z* 842). In addition, *m/z* 731 was assigned as a methylation of Sal B, and *m/z* 1022 was formed from Sal B and GSH. In general, the metabolites obtained from electrochemical oxidation of five target analytes were similar to metabolites generated from in *vitro* RLM microsomes incubations.

3.4. Comparison with previous reports

To verify, the electrochemically formed oxidation products were comparable with those obtained by *vivo* studies. In Table 1, data compare the products from the conventional in *vivo* technique under different metabolic modes (gut microflora, rat plasma, bile, urine, feces, WZS-pig urine, etc.), as well as the metabolites obtained by the EC/MS that were observed for RA, PA, Sal C, LA, Sal B. Metabolites in *vivo* studies could be deduced to derive from two types of constituents in RA of (1) bound form (methylation, sulfation etc.) and (2) ester bond hydrolysis and dehydroxylation process (caffeic acid, coumaric acid, 3,4-Dihydroxyphenyllactic acid, etc.). Metabolism of the similar EC/MS, PA, has been investigated with the determination of certain primary metabolism routes. The results of metabolism studies on PA showed that the main metabolic pathways were methylation, sulfation and glucuronidation except for the original formation. The methylated PA and the PA dimethylated sulfuric acid conjugate produced by EC/MS were similar to those reported in the publications. The metabolic reaction of Sal C in plasma and urine mainly underwent methylation and glucuronidation, and at the same time, caffeic acid was detected experimentally. In the EC/MS process, Sal C produced monomethyl Sal C

and carboxylated Sal C. Identification of rat serum, bile, plasma, urine and feces mainly resulted in monomethyl and dimethylated metabolites of LA, while EC/MS studies also confirmed the use of LA in electrochemical cells. The main methylation reaction was carried out. Due to the extensive metabolic reaction of Sal B, various methylation and sulfation reactions in rat plasma, bile, urine and feces have been reported, as well as ester bond hydrolysis and ring opening to formed LA, Danshensu, salvianolic acid A and salvianolic acid R, S, T (named by the author). In the electrochemical simulation, methylation reaction mainly occurred. The results of comprehensive reports have shown that, reactive metabolites in the components of Danshen, including methylation, sulfation, carboxylation, decarboxylation and ester bond hydrolysis, have been identified, indicating that electrochemical systems combined with mass spectrometry were an effective alternative method in *vitro* studies.

4. Conclusions

The present work clearly illustrated that EC/MS is a simple, rapid and powerful tool to evaluate the natural product transformation pathway. Reactions that could be simulated comprise straightforward oxidation of RA, PA, Sal C, LA, Sal B as well as conjugated adduct generation. The coupling of EC with MS enabled online monitoring and structure declaration of oxidation products, and was successfully compared to established in *vitro* microsomes incubation with RLM. The main metabolites of phenolic acids included methylation, sulfation, carboxylation, decarboxylation, and ester bond hydrolysis as well as various combinations of these modifications. The results demonstrated that the simple and direct online-coupled EC/MS system enabled the formation and identification of most phase I and phase II potential metabolites of phenolic acids occurring in Danshen sample, which made it one of the alternative ways for *vitro* metabolic studies.

CRediT authorship contribution statement

Juan Yang conducted all the experiments, analyzed data and wrote the manuscript. Yan Chen conducted data analysis and article modification for this research. Xiao-Ting Zhen conducted data analysis and article modification for this research. Xin Dong conducted data analysis and article modification for this research. Li-Hong Ye is responsible for conception, design, supervision and research, and guide data analysis and manuscript preparation. Hui Zheng is responsible for conception, design, supervision and research, and guide data analysis and manuscript preparation. Jun Cao is responsible for conception, design, supervision and research, and guide data analysis and manuscript preparation.

Declaration of Competing Interest

The authors declare that they have no known competing financial interests or personal relationships that could have appeared to influence the work reported in this paper.

Acknowledgements

This study was supported by the National Natural Science Foundation of China (China, 81573552), Public Welfare Research Project of Zhejiang Province (China, LGF18H280004, LGF18H280006), Hangzhou Social Development of Scientific Research projects (China, 20191203B13), Projects for Study Abroad Returnees of Hangzhou (China, 2017).

Appendix A. Supplementary data

Supplementary data to this article can be found online at https://doi.org/10.1016/j.foodchem.2020.126270.

References

Arora, T., Mehta, A. K., Joshi, V., Mehta, K. D., Rathor, N., Mediratta, P. K., & Sharma, K. K. (2011). Substitute of animals in drug research: An approach towards fulfillment of 4Rs. *Indian Journal of Pharmaceutical Sciences, 73*, 1–6.

Bel-Rhlid, R., Crespy, V., Pagé-Zoerkler, N., Nagy, K., Raab, T., & Hansen, C. E. (2009). Hydrolysis of rosmarinic acid from rosemary extract with esterases and lactobacillus johnsonii in vitro and in a gastrointestinal model. *Journal of Agricultural and Food Chemistry, 57*, 7700–7705.

Brandon, E. F. A., Raap, C. D., Meijernan, I., Beijnen, J. H., & Schellens, J. H. M. (2003). An update on in vitro test methods in human hepatic drug biotransformation research: Pros and cons. *Toxicology and Applied Pharmacology, 189*, 233–246.

Bussy, U., Chung-Davidson, Y. W., Li, K., & Li, W. M. (2014). Phase I and phase II reductive metabolism simulation of nitro aromatic xenobiotics with electrochemistry coupled with high resolution mass spectrometry. *Analytical and Bioanalytical Chemistry, 406*, 7253–7260.

Geng, Z. H., Huang, L., Song, M. B., & Song, Y. M. (2015). Cardiovascular effects in vitro of a polysaccharide from Salvia miltiorrhiza. *Carbohydrate Polymers, 121*, 241–247.

Getek, T. A., Korfmacher, W. A., McRae, T. A., & Hinson, J. A. (1989). Utility of solution electrochemistry mass spectrometry for investigation the formation and detection of biologically important conjugates of acetaminophen. *Journal of Chromatography A, 474*, 245–256.

Iyer, K. R., & Sinz, M. W. (1999). Characterization of Phase I and Phase II hepatic drug metabolism activities in a panel of human liver preparations. *Chemico-Biological Interactions, 118*, 151–169.

Jiang, X., Jin, Y., Yuan, B., Sun, S. T., Xu, P. W., & Xu, H. Y. (2012). Analysis of metabolites in vivo of compound danshen dripping pills. *Journal of Shenyang Pharmaceutical University, 29*, 126–131.

Jiang, R. W., Lau, K. M., Hon, P. M., Mak, T. C. W., Woo, K. S., & Fung, K. P. (2005). Chemistry and biological activities of caffeic acid derivatives from Salvia miltiorrhiza. *Current Medicinal Chemistry, 12*, 237–246.

Jurva, U., Wikström, H. V., & Bruins, A. P. (2000). In vitro mimicry of metabolic oxidation reactions by electrochemistry/mass spectrometry. *Rapid Communications in Mass Spectrometry, 14*, 529–533.

Jurva, U., Wikstrom, H. V., Weidolf, L., & Bruins, A. P. (2003). Comparison between electrochemistry/mass spectrometry and cytochrome P450 catalyzed oxidation reactions. *Rapid Communications in Mass Spectrometry, 17*, 800–810.

Karady, M., Novák, O., Horna, A., Strnad, M., & Doležal, K. (2011). High performance liquid chromatography-electrochemistry-electrospray ionization mass spectrometry (HPLC/EC/ESI-MS) for detection and characterization of roscovitine oxidation products. *Electroanalysis, 23*, 2898–2905.

Li, Y. G., Song, L., Liu, M., Hu, Z. B., & Wang, Z. T. (2009). Advancement in analysis of Salviae miltiorrhizae Radix et Rhizoma (Danshen). *Journal of Chromatography A, 1216*, 1941–1953.

Li, X. C., Yu, C., Lu, Y. L., Gu, Y. L., Lu, J., Xu, W., ... Wang, Y. P. (2007). Pharmacokinetics, tissue distribution, metabolism, and excretion of depside salts from salvia miltiorrhiza in rats. *Drug Metabolism & Disposition, 35*, 234–239.

Lohmann, W., Hayen, H., & Karst, U. (2008). Covalent protein modification by reactive drug metabolites using online electrochemistry/liquid chromatography/mass spectrometry. *Analytical Chemistry, 80*, 9714–9719.

Melles, D., Vielhaber, T., Baumann, A., Zazzeroni, R., & Karst, U. (2012). Electrochemical oxidation and protein adduct formation of aniline: A liquid chromatography/mass spectrometry study. *Analytical and Bioanalytical Chemistry, 403*, 377–384.

Melles, D., Vielhaber, T., Baumanna, A., Zazzeroni, R., & Karst, U. (2013). In chemico evaluation of skin metabolism: Investigation of eugenol and isoeugenol by electrochemistry coupled to liquid chromatography and mass spectrometry. *Journal of Chromatography B, 913–914*, 106–112.

Miao, J. Z., Sun, W. Y., Huang, J. Y., Liu, X. L., Li, S. M., Han, X. P., ... Sun, G. X. (2016). Characterization of metabolites in rats after intravenous administration of salvianolic acid for injection by ultra-performance liquid chromatography coupled with quadrupole-time-of-flight mass spectrometry. *Biomedical Chromatography, 30*, 1487–1497.

Mizutani, T., Yoshida, K., Murakami, M., Shirai, M., & Kawazoe, S. (2000). Evidence for the involvement of N-methylthiourea, a ring cleavage metabolite, in the hepatotoxicity of methimazole in glutathione-depleted mice: Structure-toxicity and metabolic studies. *Chemical Research in Toxicology, 13*, 170–176.

Nakazawa, T., & Ohsawa, K. (1998). Metabolism of rosmarinic acid in rats. *Journal of Natural Products, 61*, 993–996.

Sugiyama, A., Zhu, B., Takahara, M. A., Satoh, Y., & Hashimoto, K. (2002). Cardiac effects of salvia miltiorrhiza/dalbergia odorifera mixture, an intravenously applicable Chinese medicine widely used for patients with ischemic heart disease in China. *Circulation Journal, 66*, 182–184.

Sze, F. K., Yeung, F. F., Wong, E., & Lau, J. (2005). Does Danshen improve disability after acute ischaemic stroke. *Acta Neurologica Scandinavica, 111*, 118–125.

Szultka-Mlynska, M., & Buszewski, B. (2016). Electrochemistry-mass spectrometry for in-vitro determination of selected chemotherapeutics and their electrochemical products in comparison to in-vivo approach. *Talanta, 160*, 694–703.

Wang, L., Zhang, Q., Li, X. C., Lu, Y. L., Xue, Z. M., Xuan, L. J., & Wang, Y. P. (2008). Pharmacokinetics and metabolism of lithospermic acid by LC/MS/MS in rats. *International Journal of Pharmaceutics, 350*, 240–246.

Xu, M., Guo, H., Han, J., Sun, S. F., Liu, A. H., Wang, B. R., ... Guo, D. A. (2007). Structural characterization of metabolites of salvianolic acid B from Salvia miltiorrhiza in normal and antibiotic-treated rats by liquid chromatography-mass spectrometry. *Journal of Chromatography B, 858*, 184–198.

Yan, Y. T., Lai, C. J. S., Li, P., & Chen, J. (2013). Metabolites of salvianolic acid C in rats. *Journal of China Pharmaceutical University, 44*, 442–446.

Youdim, K. A., & Saunders, K. C. A. (2010). review of LC-MS techniques and high-throughput approaches used to investigate drug metabolism by cytochrome P450s. *Journal of Chromatography B, 878*, 1326–1336.

Zhang, D. L., Luo, G., Ding, X. X., & Lu, C. A. (2012). Preclinical experimental models of drug metabolism and disposition in drug discovery and development. *Acta Pharmaceutica Sinica B, 2*, 549–561.

Zhao, X., Yang, D. H., Zhou, Q. L., Xu, F., Zhang, L., Liang, J., ... Yang, X. W. (2013). Identification of metabolites in WZS-miniature pig urine after oral administration of Danshen decoction by HPLC coupled with diode array detection with electrospray ionization tandem ion trap and time-of-flight mass spectrometry. *Biomedical Chromatography, 27*, 720–735.